

Effect of Chemical Mechanisms on Deflagration to Detonation Transition and Its Application to Mechanism Reduction

Han Li^{1,3}, Tianhan Zhang^{2,3}, Zhi X. Chen^{1,3}

¹ State Key Laboratory of Turbulence and Complex Systems, Peking University
Beijing, China

² Department of Mechanics and Aerospace Engineering, SUSTech
Shenzhen, China

³ AI for Science Institute, Beijing
Beijing, China

1 Introduction

Reduced mechanisms that are well validated in homogeneous autoignition are widely adopted in detonation modelling. However, such reduced mechanisms may not be suitable for modelling deflagration to detonation transition (DDT) due to its very different characteristics from homogeneous autoignition. For instance, reactivity gradients are important for DDT, but not of concern in homogeneous autoignition. More discussion on the suitability of reduced mechanisms in detonation modelling is needed. For this purpose, first, this work uses dimethyl ether (DME) ignition as an example to investigate the effects of chemical mechanisms on deflagration to detonation transition modelling with a hot/cold spot. The observations are then applied to assist in mechanism reduction of the n-heptane detailed mechanism, in particular to assess the reduced mechanisms used for DDT modelling.

2 Methodologies

2.1 Mechanism reduction

In this work, the DRGEP method and the PFA method are used for mechanism reductions. For simplicity's sake, detailed descriptions are omitted here but can be referred to the original works [1, 2].

The DRGEP method is one of the most widely used methods for mechanism reduction. In the DRGEP method, the relation coefficient $r_{AB,p}$ along a specific reaction pathway p from species A to species B is calculated in a geometric damping way, i.e., multiplying the direct relation coefficient along p . The DRGEP coefficient R_{AB} is then defined as the maximum relation coefficient along all possible reaction pathways from A to B . If the R_{AB} is larger than a given threshold, species B will be retained to ensure the accurate prediction of target species A . Usually, fuel species, together with oxidizer, critical radicals

or products are manually selected as target species at the beginning of reduction. The PFA method is another widely used reduction method. In the PFA method, relation between a species C and a pre-selected target species D is quantified based on the flux for both the first and second generation. The first-generation flux of target species D via the species C is referred to the direct interaction of the species C in the consumption and production of target species D . The second-generation flux is referred to flux between D and C via a third reactant M , which is utilized in this work.

2.2 Numerical setup for detonation modelling

Two typical fuels for detonation research, DME and n-heptane, are considered in this study. The chemical mechanisms from Ref. [3, 4] for DME and Ref. [5] for n-heptane are used here. The transient autoignition front propagation initiated by a hot or cold spot is simulated in a one-dimensional planar configuration. The length of the computational domain is 3 cm with reflective boundary conditions on both sides. The domain is filled with stoichiometric fuel/air mixture at the pressure of 40 atm. The left side of the domain is set to be an ignition spot with a 6 mm length and a constant temperature gradient dT_0/dx (negative for hot spot, positive for cold spot). The temperature T_0 outside the ignition spot is uniform. The critical temperature gradient (CTG) at which autoignition is comparable to an acoustic time is given as:

$$\left(\frac{dT_0}{dx}\right)_c = a^{-1} \left(\frac{d\tau}{dT_0}\right)^{-1} \quad (1)$$

where a is local sound speed, τ is ignition delay time. The CTG values at given T_0 will be used for further analysis of deflagration to detonation transition (DDT).

The simulations are performed using our recently developed software DeepFlame [6], an open-source platform for reacting flow simulations. In these one-dimensional detonation simulations using DeepFlame, an adaptive mesh refinement (AMR) algorithm is implemented to refine cells in chemically intense areas (i.e., near the reaction front) with a criteria of normalized density gradient. The initial grid size here is set to 0.1 mm. The minimum mesh size after refinement is 0.0125 mm, as the maximum refinement level is set to 3. With AMR, a computational speedup of around one order of magnitude is achieved [6]. For the following n-heptane detonation, the simulation cost using the detailed mechanism is around 4000 CPU hours, while the one using the reduced mechanism is around 200 CPU hours.

3 Results and Discussions

3.1 Effect of chemical mechanisms on deflagration to detonation transition

This part utilizes two different chemical mechanisms of dimethyl ether (DME) from different sources to model the reaction front propagation from both hot spot and cold spot. One mechanism is the Zhao's mechanism with 55 species [3]. The other one is a recently developed 113-species NUIG mechanism [4]. Ignition delay times of stoichiometric DME/air mixture at 40 atm are calculated using the two mechanisms separately. Fig. 1 shows obvious difference for same initial temperatures. For example, the temperature of 1000 K falls in the negative temperature coefficient (NTC) region for the Zhao's mechanism, but not for the NUIG mechanism. To investigate the effects of the kinetic difference on detonation modelling, one-dimensional simulations of reaction front propagation ignited by a hot/cold spot are conducted using both mechanisms at 1000 K, 40 atm and stoichiometric conditions. The results are presented in Fig. 2. As can be seen, these two mechanisms exhibit very different predictions on DDT. Specifically, in the hot spot ignition, detonation develops for the NUIG mechanism and propagates from the left to the right side of the domain, while deflagration is observed for the Zhao's mechanism. Great difference has also been observed in the cold spot ignition. To explain these differences, the CTG values are calculated for the two mechanisms and plotted in Fig. 3. As can be seen, at 1000 K, the CTGs for

the two mechanisms show similar absolute values, however one is positive and the other is negative, which explains the different DDT predictions in the hot spot ignition and the cold spot ignition.

3.2 Application to mechanism reduction for detonation

The above study shows that for a same fuel, different chemical mechanisms may have very different CTG values and DDT predictions. In this section, the use of CTG values for reduced mechanism validation is proposed and tested for detonation modelling. The autoignition front propagation of stoichiometric n-heptane/air mixture with temperature gradient is simulated using the detailed chemical mechanism and two reduced mechanisms, respectively. In mechanism reduction, a 50% maximum error limit on ignition delay times is set, and two different reduction methods (i.e., DRGEP and PFA) are utilized to generate the two reduced mechanisms. The one generated by DRGEP contains 186 species and is named Reduced-1, while PFA-generated one contains 185 species and is named Reduced-2. These two mechanisms have similar number of species as well as predicting accuracy on ignition delay times as shown in Fig. 4. However, the critical temperature gradients for Reduced-1 show a much closer agreement with those of the detailed mechanism as presented in Fig. 5. It indicates that Reduced-1 should have better reproduction of the DDT and more suitable for detonation modelling, which is further proved by the results from one-dimensional detonation modelling shown in Fig. 6. It can be concluded that constraining ignition delay time is not straightforward and adequate for developing reliable reduced mechanisms for detonation modelling. Instead, CTG values are important for DDT, and are suggested to be used as an indicator for mechanism validations.

3.3 Sensitivity analysis

To further analyze the difference between ignition delay and CTG values from a chemical kinetic perspective, a brutal-force sensitivity analysis of CTG values and ignition delay with respect to reaction rate constants is conducted at the operating condition of $\phi=1.0$, $P=40\text{atm}$ and $T=900\text{K}$. The Reduced-1 mechanism is taken as an example for the analysis here. Table 1 lists the top 10 sensitive reactions and their sensitivity coefficients S_i . As can be observed, the isomerization reactions of C7H15O2-2 and its isomers have a significant influence on ignition delay, while the hydrogen abstraction reactions of NC7H16 plays a more crucial role in affecting CTG values. These findings further emphasize that ignition delay metrics alone are insufficient when evaluating chemical mechanisms in DDT modelling.

Table 1 Normalized sensitivity coefficient of CTG (left) and ignition delay (right) with respect to reaction rate constants.

CTG sensitivity analysis			ignition delay sensitivity analysis	
No.	Reaction	S_i	Reaction	S_i
1	$\text{HO}_2 + \text{NC}_7\text{H}_{16} \Rightarrow \text{C}_7\text{H}_{15}\text{-}2 + \text{H}_2\text{O}_2$	0.61	$\text{C}_7\text{H}_{15}\text{O}_2\text{-}2 \Leftrightarrow \text{C}_7\text{H}_{14}\text{OOH}_2\text{-}4$	-0.39
2	$\text{HO}_2 + \text{NC}_7\text{H}_{16} \Rightarrow \text{C}_7\text{H}_{15}\text{-}3 + \text{H}_2\text{O}_2$	0.51	$\text{H}_2\text{O}_2 (+\text{M}) \Leftrightarrow 2 \text{OH} (+\text{M})$	-0.31
3	$\text{H}_2\text{O}_2 (+\text{M}) \Leftrightarrow 2 \text{OH} (+\text{M})$	0.44	$\text{C}_7\text{H}_{15}\text{O}_2\text{-}3 \Leftrightarrow \text{C}_7\text{H}_{14}\text{OOH}_3\text{-}5$	-0.30
4	$\text{C}_7\text{H}_{14}\text{OOH}_2\text{-}4 + \text{O}_2 \Rightarrow \text{C}_7\text{H}_{14}\text{OOH}_2\text{-}4\text{O}_2$	0.43	$\text{C}_7\text{H}_{14}\text{OOH}_2\text{-}4 + \text{O}_2 \Rightarrow \text{C}_7\text{H}_{14}\text{OOH}_2\text{-}4\text{O}_2$	-0.23
5	$\text{C}_7\text{H}_{14}\text{OOH}_2\text{-}4\text{O}_2 \Rightarrow \text{C}_7\text{H}_{14}\text{OOH}_2\text{-}4 + \text{O}_2$	-0.40	$\text{C}_7\text{H}_{14}\text{OOH}_2\text{-}4\text{O}_2 \Leftrightarrow \text{NC}_7\text{KET}_{24} + \text{OH}$	-0.23
6	$\text{C}_7\text{H}_{14}\text{OOH}_2\text{-}4\text{O}_2 \Leftrightarrow \text{NC}_7\text{KET}_{24} + \text{OH}$	0.36	$\text{C}_7\text{H}_{14}\text{OOH}_2\text{-}4\text{O}_2 \Rightarrow \text{C}_7\text{H}_{14}\text{OOH}_2\text{-}4 + \text{O}_2$	0.22
7	$\text{HO}_2 + \text{NC}_7\text{H}_{16} \Rightarrow \text{C}_7\text{H}_{15}\text{-}4 + \text{H}_2\text{O}_2$	0.31	$\text{C}_7\text{H}_{15}\text{O}_2\text{-}4 \Leftrightarrow \text{C}_7\text{H}_{14}\text{OOH}_4\text{-}2$	-0.21
8	$\text{NC}_7\text{H}_{16} + \text{OH} \Rightarrow \text{C}_7\text{H}_{15}\text{-}3 + \text{H}_2\text{O}$	-0.28	$\text{C}_7\text{H}_{15}\text{O}_2\text{-}1 \Leftrightarrow \text{C}_7\text{H}_{14}\text{OOH}_1\text{-}3$	-0.19
9	$\text{C}_7\text{H}_{14}\text{OOH}_3\text{-}5 + \text{O}_2 \Rightarrow \text{C}_7\text{H}_{14}\text{OOH}_3\text{-}5\text{O}_2$	0.25	$\text{C}_7\text{H}_{15}\text{O}_2\text{-}2 \Leftrightarrow \text{C}_7\text{H}_{14}\text{-}2 + \text{HO}_2$	0.18
10	$\text{C}_7\text{H}_{14}\text{OOH}_4\text{-}2 + \text{O}_2 \Rightarrow \text{C}_7\text{H}_{14}\text{OOH}_4\text{-}2\text{O}_2$	0.24	$2 \text{HO}_2 \Rightarrow \text{H}_2\text{O}_2 + \text{O}_2$	0.17

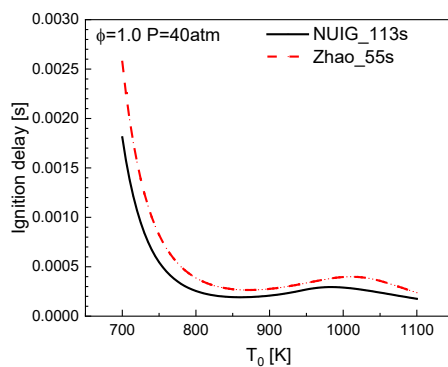


Figure 1: Ignition delay times of stoichiometric DME/air mixture predicted by the NUIG mechanism and Zhao's mechanism.

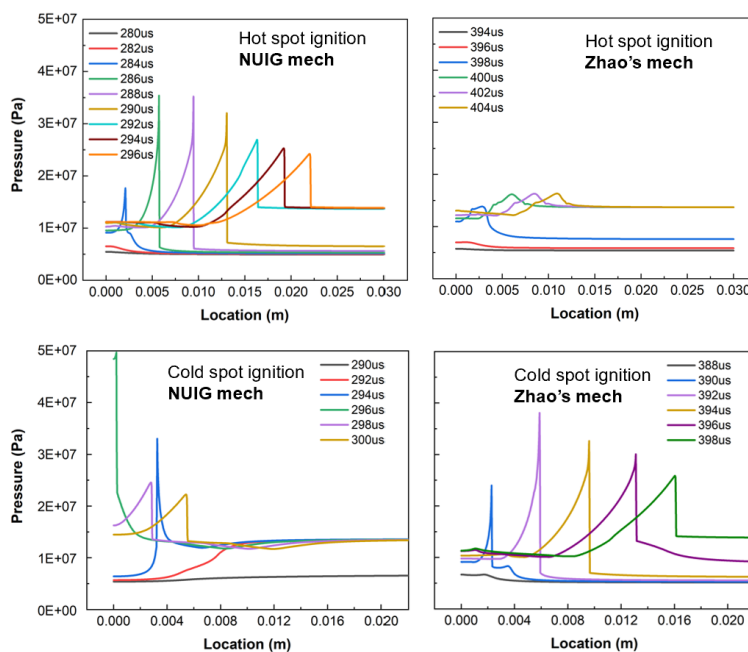


Figure 2: Temporal evolution of pressure for $T_0 = 1000$ K, $x_0 = 6$ mm in hot spot ignition with a temperature gradient of 3000 K/m (upper) and cold spot ignition with a temperature gradient of 5000 K/m (lower).

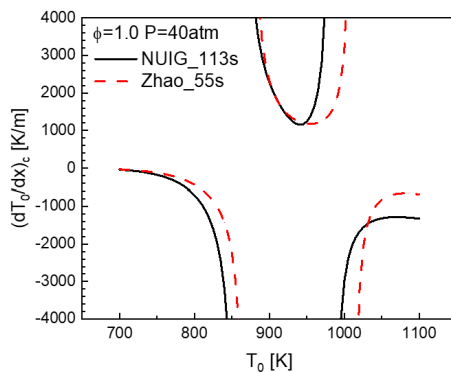


Figure 3: Critical temperature gradient as a function of initial temperature for stoichiometric DME/air mixture.

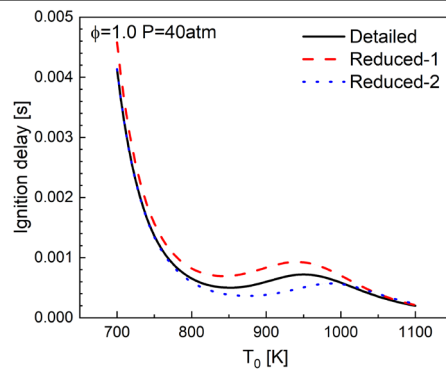


Figure 4: Ignition delay time of stoichiometric n-heptane/air mixture predicted by the detailed mechanism and the two reduced mechanisms.

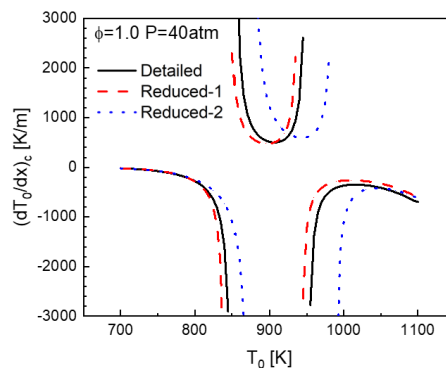


Figure 5: Critical temperature gradient as a function of initial temperature for stoichiometric n-heptane/air mixture.

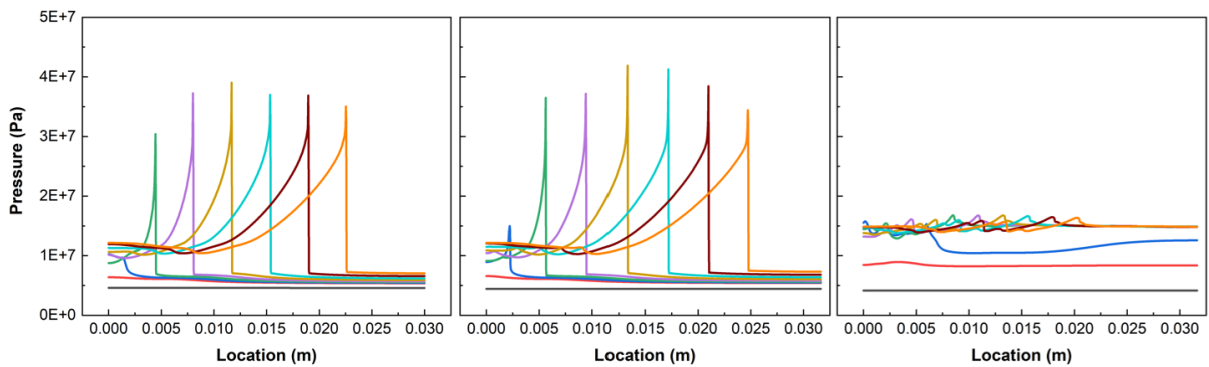


Figure 6: Temporal evolution of pressure for $T_0 = 900$ K, $x_0 = 6$ mm in cold spot ignition with a temperature gradient of 3000 K/m predicted by the detailed mechanism (left), the reduced-1 (middle) and the reduced-2 (right).

4 Conclusions

In the reduction of detailed chemical mechanisms, ignition delay time is often used as a main constraining metric for the error limitations of reduced mechanisms. However, two reduced mechanisms with similar ignition delay prediction errors can have very different values of critical temperature gradient, which is more relevant for modelling DDT. In this work, we firstly simulated autoignition front propagation of a stoichiometric DME/air mixture with temperature gradient to demonstrate that chemical mechanisms have a great influence on the CTG values and the predictions on DDT. Later, we introduced the CTG values as a validation metric for detonation mechanism reduction. Two different reduced mechanisms, with comparable sizes and accuracy on autoignition prediction, are generated and utilized to prove that the introduction of CTG metric in mechanism reduction helps to validate the reduced mechanisms for detonation modelling.

This work also indicates that ignition delay metrics might not be sufficient when evaluating detailed mechanisms for reproducing DDT from experiments. Since experimental measurement of CTG values is not straightforward and can even be prohibitive, qualitative experiments on DDT may help to validate detailed mechanisms and therefore deserve significant attention.

Acknowledgment

The work is supported by the National Science Foundation (Grant No. 52276096 and No. 92270203) and the Fundamental Research Funds for the Central Universities of China. Part of the numerical simulations was performed on the High Performance Computing Platform of CAPT of Peking University.

References

- [1] P. Pepiot-Desjardins, H. Pitsch. (2008). An efficient error-propagation-based reduction method for large chemical kinetic mechanisms. *Combust. Flame* 154 67-81.
- [2] W. Sun, Z. Chen, X. Gou, Y. Ju. (2010). A path flux analysis method for the reduction of detailed chemical kinetic mechanisms. *Combust. Flame* 157 1298-1307.
- [3] Z. Zhao, M. Chaos, A. Kazakov, F.L. Dryer. (2008). Thermal decomposition reaction and a comprehensive kinetic model of dimethyl ether. *Int. J. Chem. Kinet.* 40 1-18.
- [4] U. Burke, K.P. Somers, P. O'Toole, C.M. Zinner, N. Marquet, G. Bourque, E.L. Petersen, W.K. Metcalfe, Z. Serinyel, H.J. Curran. (2015). An ignition delay and kinetic modeling study of methane, dimethyl ether, and their mixtures at high pressures. *Combust. Flame* 162 315-330.
- [5] M. Mehl, W.J. Pitz, C.K. Westbrook, H.J. Curran. (2011). Kinetic modeling of gasoline surrogate components and mixtures under engine conditions. *Proc. Combust. Inst.* 33 193-200.
- [6] R. Mao, M. Lin, Y. Zhang, T. Zhang, Z.-Q.J. Xu, Z.X. Chen. (2022). DeepFlame: A deep learning empowered open-source platform for reacting flow simulations. *arXiv:2210.07094*.